

# Quantification of delta and fluvial fan channel networks reveals distinct formative processes

## Authors

Luke Gezovich<sup>1</sup>, Piret Plink-Björklund<sup>1</sup>, Jack Henry<sup>1,2</sup>

<sup>1</sup> Colorado School of Mines, Geology & Geologic Engineering, 1500 Illinois Street, Golden, CO, 80401

<sup>2</sup> Rice University, Earth, Environmental and Planetary Sciences, 6100 Main St., Houston, TX, 77005-1827

## Key Points

1. There are quantifiable morphometric differences in delta and fluvial fan channel networks.
2. These differences reflect distinct morphodynamics of these landforms.
3. Deltas and fluvial fans adjust differently to global change.

## **Abstract**

Deltas and fluvial fans are two fan-shaped landforms with complex channel networks. Deltas always occur where rivers enter a standing body of water, such as lakes or oceans. Fluvial fans are inland terrestrial landforms that may form thousands of kilometers from shorelines. Fluvial fans may however also reach lakes and oceans. The current state of knowledge lacks understanding of their morphometric differences or recognition criteria, despite their socioeconomic significance, vulnerability to natural hazards, and important differences in how these landforms respond to global climate change. Moreover, numerous fan-shaped landforms with channel networks have been identified on other planetary bodies, such as Mars and the Saturn's moon Titan, where deltas are important indicators of paleo-shorelines and offer attractive targets for mission sites due to their habitability and high biosignature preservation potential. Here we review the known morphometrics of delta and fluvial fan channel networks, and the differences in their formative processes, and develop morphometric criteria for distinguishing deltas and fluvial fans. We present an ensemble of quantitative metrics that distinguish deltas and fluvial fans and test these criteria on 80 modern channel networks on Earth. Our results improve mechanistic understanding of the fluvial record and delta evolution, provide criteria for accurate recognition of these landforms on planetary bodies and in the sedimentary record, and explain differences in their vulnerabilities to global change.

## **Plain Language Summary**

Deltas and fluvial fans are fan-shaped landforms that exhibit complex river channel networks. Deltas form when a river enters a body of water, such as a lake or ocean and are fan shaped. Fluvial fans are another fan-shaped landform which may or may not form along a body of water, and form from repeated lateral shifts in channels across the fan surface. Geoscientists currently lack the ability to distinguish between their channel networks based on channel metrics like channel lengths, widths, and branching angles. It is important to distinguish between deltas and fluvial fans as each has different vulnerabilities to natural hazards and climate change. Furthermore, numerous fan shaped landforms have been identified on Mars where deltas are indicators of ancient shorelines. Here, we review the differences in distributary channel networks in deltas and fluvial fans and discuss the sedimentological processes responsible for their formation. We present quantitative metrics that can be used to distinguish deltas and fluvial fans and test these criteria on 40 modern delta and 40 fluvial fan channel networks. Our results improve our understanding of delta and fluvial fan channel networks and provide recognition criteria for these landforms in the sedimentary record and on other planets.

**Index Terms**

Geomorphology (general) | Geomorphology (fluvial) | River channels | GIS Science | Surfaces

**Keywords**

Delta | Fluvial Fan | Surface Processes | Geomorphology | Channel Networks

## 1. Introduction

River deltas are landforms which form where rivers enter lakes or oceans. Their morphology results from an intricate balance between sediment erosion and deposition from river, tide, and wave processes (Galloway, 1975; Orton & Reading, 1993). It is hard to overestimate the significance of deltas. Deltas are home to over half a billion people, host rich and biodiverse ecosystems, and function as both economic and agricultural hubs (Saito et al., 2007; Tejedor et al., 2015). Deltas are also global change hotspots highly vulnerable to increasing urbanization and climate change which aggravate coastal hazards and causes sea level rise (e.g. Giosan et al., 2014; Syvitski et al., 2009). Reduced water and sediment supply due to river damming and artificial levees have further threatened deltas (e.g. Blum & Roberts, 2009; Giosan et al., 2014; Nienhuis et al., 2020; Paola et al., 2011; Syvitski et al., 2009). Deltas contain a complex network of distributary channels (Figure 1) that disperse water, sediment, nutrients, and carbon from upstream sources to downstream wetlands and coastlines (Saito et al., 2007).

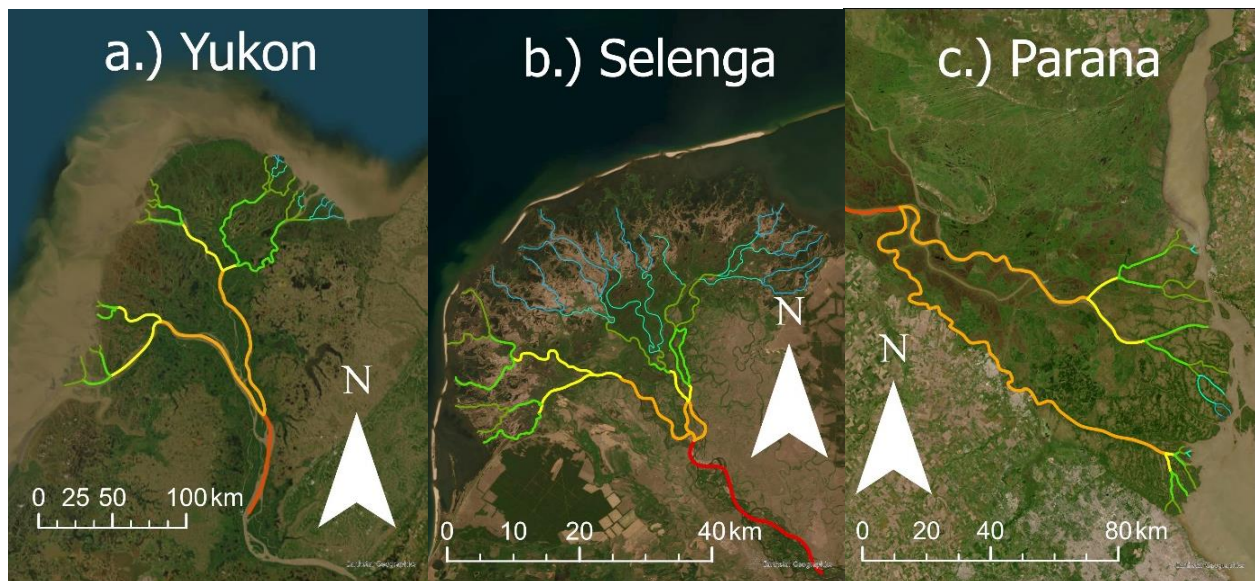


Figure 1: Examples of delta distributary channel networks: (a) Yukon, (b) Selenga, and (c) Parana.

Fluvial fans are a relatively newly acknowledged type of fluvial system (Ventra & Clarke, 2018), and they are also a landform with a complex network of channels (Figure 2). They are distinct from deltas in that they are inland terrestrial landforms, although they may reach the shorelines of oceans or lakes (Figure 2). Fluvial fans are predominantly controlled by upstream morphodynamics (Leier et al., 2005; North & Warwick, 2007). They are therefore less sensitive to sea-level rise and coastal hazards, but highly sensitive to the water and sediment supply changes driven by global change (Assine et al., 2014; Hansford & Plink-Björklund, 2020; Leier et al., 2005). Fluvial fans are common on Earth and form in many different climates and tectonic settings (Hartley et al., 2010; Ventra & Clarke, 2018; Weissman et al., 2010), and in places cover large surface areas and generate channel networks hundreds of kilometers wide (Ventra & Clarke, 2018). Fluvial fan formation is promoted by a high sediment flux (North & Warwick, 2007), and by fluctuations in river discharge because intense and intermittent precipitation promotes marked seasonal and interannual hydrological changes, leading to variable discharge regimes and exceptional flood events (Hansford & Plink-Björklund, 2020; Leier et al., 2005). Thus, fluvial fan rivers are highly dynamic landforms and likely to experience hazardous floods, such as are common in Kosi Fluvial Fan (Rajiv Sinha, 2009; Syvitski & Brakenridge, 2013).

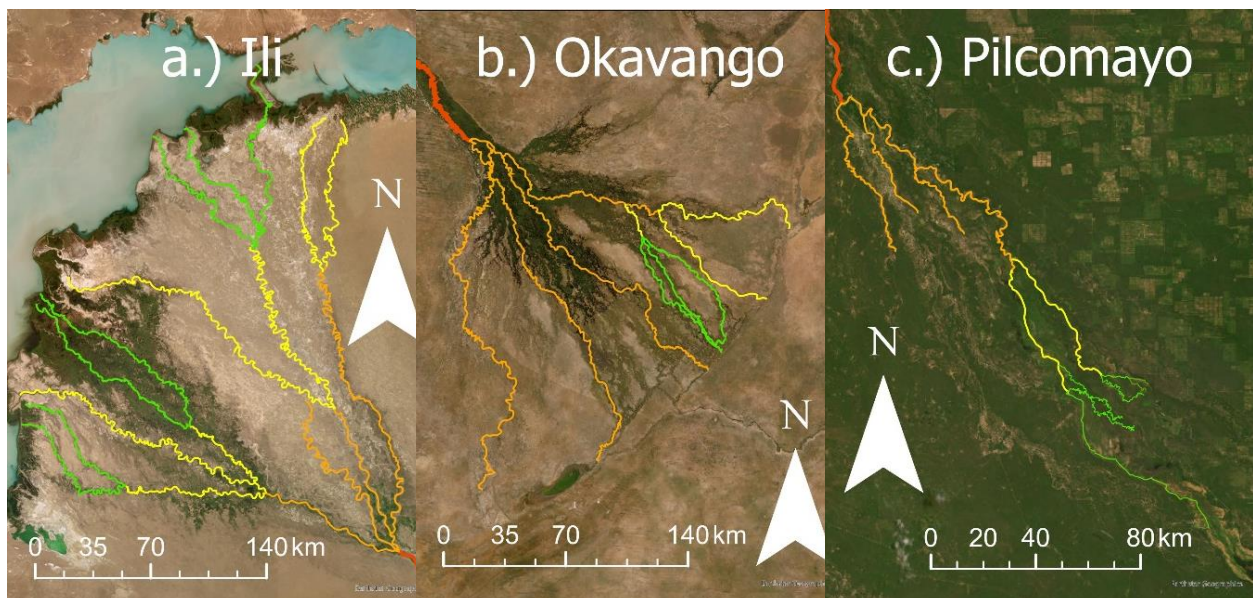


Figure 2: Examples of fluvial fan networks: (a) Ili, (b) Okavango, and (c) Pilcomayo.

Currently, there are no recognition criteria for these two landforms, despite their socioeconomic significance, vulnerability to natural hazards, and important differences in how they respond to global change. Moreover, numerous fan-shaped landforms featuring channel networks have been identified on other planetary bodies, such as Mars (Malin & Edgett, 2015; Ori et al., 2000; Wood, 2006), and the Saturn's moon Titan (Radebaugh et al., 2018; Wall et al., 2010; Witek & Czechowski, 2015). Deltas on planetary bodies are important indicators of paleo-shorelines and have been utilized to reconstruct the shorelines and water levels of ancient oceans on Mars (di Achille & Hynek, 2010). Deltas along shorelines offer attractive targets for mission sites due to their habitability and high biosignature preservation potential, as exemplified by the selection for the Perseverance MRS landing site in the Jezero Crater (Farley et al., 2020). However, global paleo-shoreline reconstructions on Mars have returned mixed results (De Toffoli et al., 2021). Such mixed results may be a consequence of misinterpreting fluvial fan channel networks that may occur thousands of kilometers inland from shorelines as deltaic (Farley et al., 2020).

Over time, the accumulation of biogenic and sedimentary materials distributed via channel networks contributes to the construction of stratigraphy. Fluvial fans and deltas are net depositional systems because both are characterized by spatially diminishing water surface slopes that reduce sediment transport capacity, thereby producing spatiotemporal convergence and deposition of sediment (Ganti et al., 2014). Consequently, in addition to their socioeconomic significance, both landforms contribute significantly to the stratigraphic record, and their deposits may be used to decipher past environmental conditions. Especially, as most of the terrestrial sedimentary record is suggested to be formed by fluvial fans (Weissman et al., 2010). Due to their sensitivity to precipitation pattern and sediment flux (Fontana et al., 2014; Hansford & Plink-Björklund, 2020; Leier et al., 2005) they are important indicators of past climate change, and particularly changes in precipitation intensity and intermittency (Carmichael et al., 2017; Hansford & Plink-Björklund, 2020; Schmitz & Pujalte, 2007). High deposition rates in fluvial fans

promote the preservation of climate change signals in the sedimentary record, and the rapid lateral distribution of sediment due to frequent avulsions makes climate proxy records less sensitive to sampling location and fluvial fans especially valuable as climate change archives (Trampusch & Hajek, 2017). For instance, the Kosi River has avulsed approximately every 7 years between 1760 and 1960 and has shifted across the whole fan surface over just 200 years (Chakraborty et al., 2010).

We propose that distinguishing deltas and fluvial fans is of socioeconomic importance to better understand the effects of global change on these widely distributed landforms more accurately, as well as for interpreting the stratigraphic record, and correctly recognizing these landforms on other planetary bodies. Geoscientists currently lack specific morphological criteria that can be used to distinguish the channel networks in fluvial fans and deltas. Much work has been done to establish quantitative morphological criteria for describing deltaic channel networks, and to link these characteristics to theory (e.g., Coffey & Shaw, 2017; Edmonds & Slingerland, 2007; Fagherazzi et al., 2015), but similar work on fluvial fans is missing. We propose to use such channel network morphometric criteria to differentiate deltas and fluvial fans. This review covers the conceptual differences in delta and fluvial fan network morphodynamics, defines criteria based on quantitative morphometrics to distinguish fluvial fan and delta channel networks, and tests these criteria on 40 deltas (Table 1) and 40 fluvial fans (Table 2) from across the globe Figure 3. This work serves to improve our mechanistic understanding of fluvial fan and delta evolution to promote sustainability of these resources, and accurate recognition on planetary bodies and in the sedimentary record.

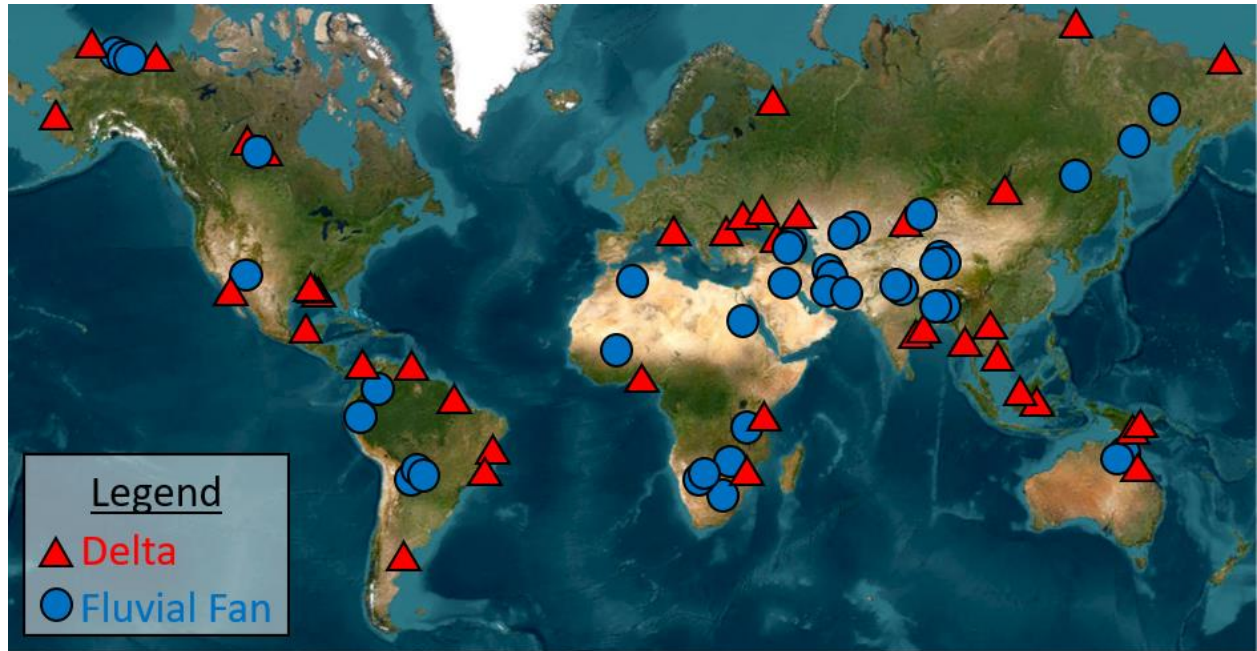


Figure 3: Global distribution of 40 deltas and 30 fluvial fans included in this study.

## **2. Morphodynamics of Delta and Fluvial Fan Channel Networks**

The nature of channel networks is dependent on distinct morphodynamic processes (Edmonds & Slingerland, 2007; Fagherazzi et al., 2015; Tejedor et al., 2015). Below we analyze differences in delta and fluvial fan morphodynamics, review the existing morphometric criteria for analyzing channel networks, and propose criteria applicable for differentiating channel networks in deltas and fluvial fans.

### **a. River Deltas**

Deltas (Figure 1) always form where the mouth of a river enters a standing body of water. Here, the transport capacity of the turbulent jet decreases, and the “parent” stream jet flow experiences both lateral and bed friction, causing the flow to decelerate and rapidly expand laterally (Bates, 1953; Wright, 1977; Edmonds & Slingerland, 2007; Jerolmack & Swenson, 2007). As a result, the transport capacity of the turbulent jet decreases and sediment is deposited as a river mouth bar basinward of the river mouth (Edmonds & Slingerland, 2007). This mouth bar growth eventually leads to a bifurcation, defined as distinct division of channelized flow, where a single channel (parent channel) branches into two or more channels (daughter channels) (Axelsson, 1967; Coffey & Shaw, 2017) (Figure 4a). The daughter channels are separated by a bar, island, or shallow bay where sediment transport is significantly reduced or nonexistent, and flow is unchannelized (Coffey & Shaw, 2017). Mouth bar deposition and resultant channel bifurcation repeats multiple times leading to the seaward advancement of the shoreline and the construction of a delta distributary channel network (Edmonds & Slingerland, 2007; Olariu & Bhattacharya, 2006) (Figure 4a).

Deltas also experience avulsions – channel shifts that occur via “channel jumping” about a spatial node (Slingerland & Smith, 2004). Deltaic avulsions occur within a region of high-water surface slope variability caused by backwater hydrodynamics that are characterized by spatial flow deceleration and deposition at low flows, and flow acceleration and bed scour at high flows (Chatanantavet & Lamb, 2014; Lamb et al., 2012), and set the location for avulsion on deltas (Chatanantavet et al., 2012). Like bifurcations, avulsions in deltas are thus controlled by hydrodynamics in a receiving basin. As a result, the delta lobe size is consistent, and the avulsion node migrates downstream commensurate with the shoreline progradation (Ganti et al., 2014).

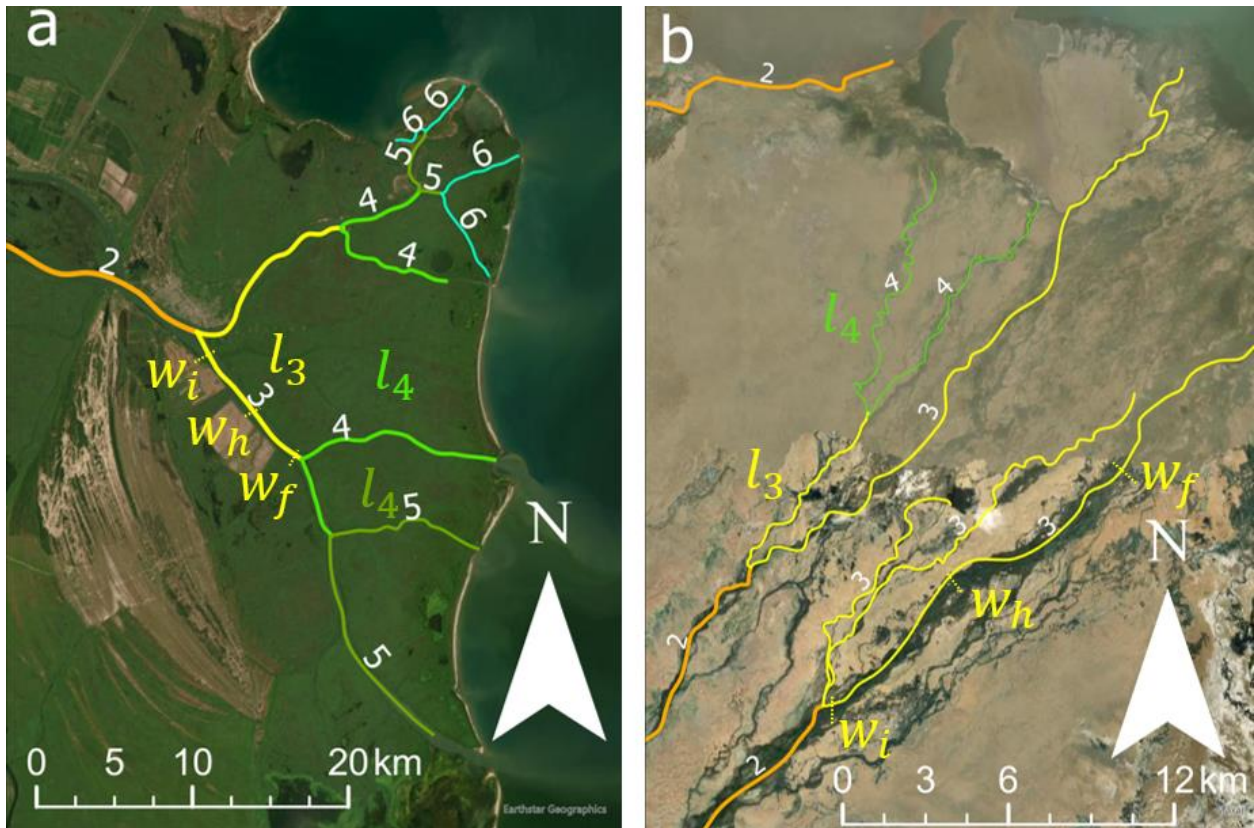


Figure 4: Illustration of channel length ( $l$ ) and width ( $w$ ) measurement methods in (a) Danube delta and (b) Dzavhan Gol fan.  $w_i$  = initial width measurement,  $w_h$  = halfway/midpoint width measurement,  $w_f$  = final width measurement.  $l_n$  corresponds to channel length as recorded in ArcGIS. White numbers and color-coded channels correspond to channel bifurcation or divergence/cross-over order.

Delta channel network topology is generated predominantly by bifurcation around a river mouth bar (Edmonds & Slingerland, 2007). Deltaic avulsions only episodically rearrange the depocenter at the delta lobe scale, whereas the considerably more frequent bifurcations determine the nature of the delta channel networks (Bentley et al., 2016). The resultant delta channel networks exhibit a tendency to consistently self-organize (Edmonds et al., 2011; Fagherazzi et al., 2008), and have a fractal pattern of decreasing channel widths and lengths associated with increasing bifurcation orders (Edmonds & Slingerland, 2007; Seybold et al., 2007; Wolinsky et al., 2010) (Figure 4a). These trends in channel widths are consistent with hydraulic geometric scaling patterns; as the discharge of a parent channel divides into the discharge for two resultant daughter channels, the daughter channel dimensions decrease as they scale with bankful discharge (Edmonds & Slingerland, 2007). Channel lengths decrease downstream, because with each successive bifurcation the jet momentum flux and consequent average grain transport distance decrease downstream, causing new mouth bar deposition and accompanying bifurcations to occur closer to the previous bifurcation node for a given channel (Edmonds & Slingerland, 2007) (Figures 4a and 5a).

The nature of delta channel networks is further affected by basinal processes, such as wave and tide actions (Geleynse et al., 2011; Jerolmack & Swenson, 2007; Leonardi et al., 2013). The relative strength of river, wave, and tide processes determines whether deltas are river, wave, or tide influenced or dominated (Galloway, 1975; Nienhuis et al., 2020). Tide-influenced deltas exhibit fractal channel network patterns (Marciano et al., 2005), but the combined effect of tidal discharge amplitude and river discharge determine the formation of channels and mouth bars (Marciano et al., 2005; Nienhuis et al., 2018; Shaw & Mohrig, 2014). As a result, in tide-influenced deltas distributary channels widen seaward due to tidal erosion (Langbein, 1963; Nienhuis et al., 2018; Wright et al., 1973). Sediments from the distributary mouth are reworked into longitudinal bars perpendicular to the coast, removing sediment from river mouth and reducing bifurcations (Leonardi et al., 2013). The dominance of tidal discharge

amplitude over river discharge results in tide-dominated deltas (Nienhuis et al., 2018) that commonly contain only two to three distributary channels, which exhibit significant seaward widening, separated by elongate bars (Leonardi et al., 2013). Similarly, wave-dominated deltas exhibit few if any channel bifurcations due to wave erosion of shorelines and efficient shore-parallel redistribution of sediment (Anthony, 2015; Jerolmack & Swenson, 2007; Nardin et al., 2013). Consequently, wave and tide-dominated deltas have a distinctly different morphology from river dominated deltas and fluvial fans. Only river-dominated deltas that maintain mouth bar growth and resultant bifurcations are considered in this study. However, we included some deltas that exhibit some wave or tide influence or both (Table 1).

Another morphological characteristic of river delta channel networks is the angle at which distributary channels bifurcate (Figure 5a) (Coffey & Shaw, 2017). There is a similar dendritic morphology in tributary networks at confluences and distributary networks at bifurcations (Coffey & Shaw, 2017). The resultant theoretical bifurcation angle is  $72^\circ$  (Coffey & Shaw, 2017), which in tributary systems arises from diffusive groundwater flow (Devauchelle et al., 2012). Testing of this concept on 9 modern deltas and on experimental deltas reports bifurcation angles of  $70.4^\circ \pm 2.6^\circ$  in natural deltas and  $68.3^\circ \pm 8.7^\circ$  in experimental deltas (Coffey & Shaw, 2017). Confluence angles in tributary networks in arid climates have been suggested to differ due to insufficient groundwater flow (Seybold et al., 2017). Bifurcation angles in arctic deltas may be modified by higher levees able to constrain channel flow thus reducing the ability of a channel to bifurcate (McCloy, 1970a).

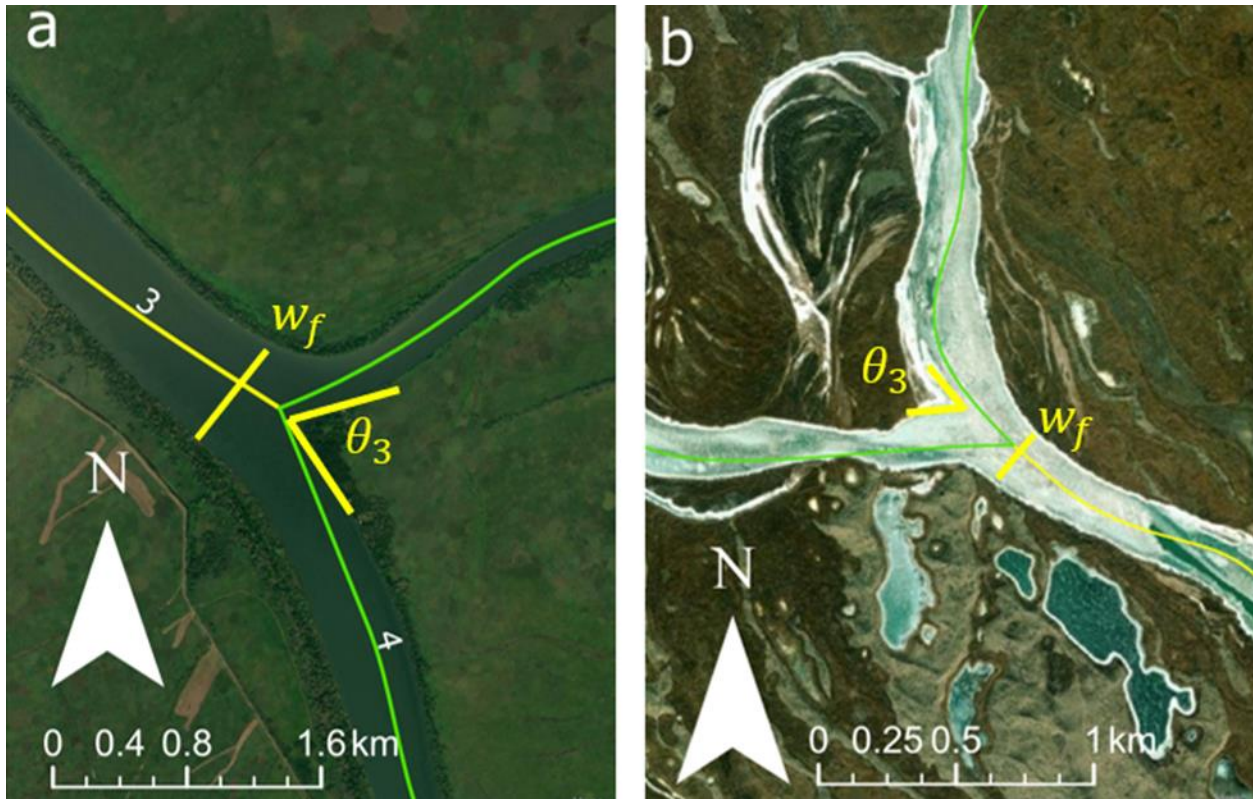


Figure 5: Illustration of (a) bifurcation angle measurement in deltas, and (b) divergence/crossover angle measurement in fluvial fans.  $w_f$  = final width measurement set as the length of two limbs that track along the edges of the mouth bar.  $\theta_n$  corresponds to the bifurcation or divergence/cross-over order.

## b. Fluvial Fans

Fluvial fans build via nodal river avulsions that originate primarily at the fan apex (Assine, 2005; Chakraborty et al., 2010; North & Warwick, 2007, Moscariello, 2018; Plink-Björklund, 2021; Ventra & Clarke, 2018), where channel bed and water surface slopes reduce, producing a lower sediment transport capacity (Jones & Schumm, 1999; Slingerland & Smith, 2004). Fluvial fans are also referred to as “wet” fluvial-dominated alluvial fans (Schumm, 1977), megafans (e.g. Singh et al., 1993) or distributive fluvial systems (DFS) (Weissman et al., 2010). The DFS concept encompasses both alluvial and fluvial fans. Alluvial fans are constructed by sediment gravity flow and sheet-flood processes and do not form constructional channel networks (Blair & McPherson, 1994). Alluvial fans are thus not considered further in this work.

In contrast to deltas where bifurcations and avulsions are controlled by hydrodynamics near a receiving basin of standing water (Chatanantavet et al., 2012; Ganti et al., 2014), fluvial fan river nodal avulsions are driven by a topographic slope break at the apex (Ganti et al., 2014). A consequence of this is increased in-channel sediment aggradation and the increased likelihood of avulsion at that location (Parker et al., 1998). This is due to high channel bed aggradation rates that are considerably higher than on the surrounding floodplains (Pizzuto, 1987) which cause channel superelevation that triggers river avulsions (Bryant et al., 1995; Mohrig et al., 2000). As this slope break controls the location of fluvial fan deposition, fluvial fans have an avulsion node that is topographically pinned (Ganti et al., 2014). Some avulsions also occur at downstream locations related to crevassing (Assine, 2005; Chakraborty et al., 2010; Donselaar et al., 2013) (Figure 2).

Thus, fluvial fan channel networks form from repeated avulsions, where new channel positions are superimposed on paleo-channel positions, and where they cross, they create the appearance of bifurcations (North & Warwick, 2007) (Figure 5b). Fluvial fan channel networks are thus paleochannel networks rather than active channel networks like in deltas (Chakraborty et al., 2010; North & Warwick, 2007). Although partial avulsions also occur where multiple channels can be active at the same time, especially during major river floods, these partial avulsions are also governed by channel bed superelevation (Bryant et al., 1995; Mohrig et al., 2000), rather than bifurcation around mouth bars.

Another reason for apparent bifurcations that were originally suggested as the mechanism for fluvial fan formation (e.g. Friend, 1978; Kelly & Olsen, 1993) is the downstream decrease in channel width documented in modern and ancient fluvial fans (Nichols, 1987; Kelly & Olsen, 1993; Nichols & Fisher, 2007; Weissman et al., 2010; Davidson et al., 2013; Owen et al., 2015; Wang & Plink-Björklund, 2019; Hansford & Plink-Björklund, 2020), due to discharge losses to floodplain processes, infiltration into the loose sediments of the fan, and evapotranspiration (DeCelles & Cavazza, 1999; Horton & Decelles, 2001; Hartley et al., 2010; Weissman et al., 2010; Davidson et al., 2013). However, some fluvial fan channels have also

been shown to widen downstream (Hansford & Plink-Björklund, 2020), possibly due to changes in channel planform or aspect ratio, discharge contribution from groundwater, or discharge capture from adjacent rivers (Chakraborty et al., 2010; Davidson et al., 2013).

### **c. Morphometric Criteria for Delta and Fluvial Fan Channel Networks**

Based on the above morphodynamic differences in delta and fluvial fan channel networks, we hypothesize that these morphometric differences can be quantified, because river-dominated delta channel networks display downstream decreasing channel widths and lengths with increasing bifurcation orders (Edmonds & Slingerland, 2007; Seybold et al., 2007; Wolinsky et al., 2010), and display average bifurcation angles of approximately  $72^\circ$  (Coffey & Shaw, 2017). In contrast, these morphometric relationships are not present in fluvial fans, because the channel networks are built by nodal avulsions, where paleochannels converge, diverge, or cross over. Below, we will utilize these morphometric criteria and apply them to 40 delta and 40 fluvial fan landforms with channel networks. We will further analyze differences in channel morphometrics in tide and wave-influenced deltas, as well as in channel networks from different climates (especially in arid and polar climates). We will also include datasets where fluvial fans enter lakes or oceans, and small deltaic networks form along the fluvial fan front.

### **3. Methods**

#### **a. Channel Order**

To establish channel order in channel networks we follow the methodology of Dong et al. (2016) which utilizes channel bifurcation patterns. This method follows a simple rule: bifurcation produces increasing downstream channel orders through channels that branch. These resultant channels must not merge downstream to be considered a true bifurcation. Channel order is based on an individual channel segment's location with respect to bifurcations. When a first order channel bifurcates, two second order channels are created downstream. When these two channels bifurcate then two new pairs of channels form, etc. (Figures 4a and 5a). Identification of bifurcation nodes follows the methodology of Edmonds et al. (2011), such that the first order bifurcation for a river channel is the first bifurcation that channel undergoes (Figures 4a and 5a). Although these methods were developed for deltaic channel networks, in this work they are also applied to fluvial fan networks (Figures 4b and 5b), although the origin of the apparent bifurcation angles is due to convergence, divergence and crossover of paleo-channel locations. In essence, we focus on the morphology of the channel networks and measure the visible angles between channels or paleo-channels independent of their origin (Figures 4b and 5b).

#### **b. Channel Length and Width Measurements**

Channel length and width measurements follow methods from Edmonds and Slingerland (2007) such that a channel length is the distance between two bifurcation nodes in deltas and between divergence or crossover angles in fluvial fans (Figure 4). The width of a channel is recorded as the average of three width measurements: one immediately after a bifurcation node ( $W_i$ ), one immediately before the next bifurcation node ( $W_f$ ), and one halfway between these two points in the channel ( $W_h$ ) (Figure 4). Widths were not measured in locations with submerged bars, nor in locations where a channel splits but later merges again downstream. Channel lengths ( $L$ ) are measured between two consequent bifurcation

or divergence/crossover nodes (Figure 5). Channel lengths and widths are then normalized using the initial channel order 1 average width (Edmonds & Slingerland, 2007). Thus, for first order channels the normalized channel width is always equal to one. The first order channel lengths were measured between the last occurrence of tributaries and the first bifurcation or divergence/crossover node.

#### **c. Channel Bifurcation and Divergence/Crossover Angle Measurement**

To quantify channel bifurcation angles in deltas we follow the methodology of Coffey and Shaw (2017). This methodology determines the angle of the mouth bar formed at the end of an upstream channel (Figure 5a). The final channel width directly upstream of a bifurcation is measured as a “parent” channel width. This parent channel width is set as the length for two limbs of an angle that track along the edges of the mouth bar-water contact to calculate a bifurcation angle (Coffey & Shaw, 2017) (Figure 5a). This same methodology was applied to fluvial fans, although the angles between two paleochannels are crossover angles between paleo-channels or channel splitting due to partial avulsions (Figure 5b). Due to tidal effects, channels in tide-influenced deltas may bifurcate into three separate channels instead of two, referred to as trifurcations (Leonardi et al., 2013), and are included in this dataset.

#### **d. Global Delta and Fluvial Fan Channel Network Database**

To test the applicability of the above methods, we selected previously studied and defined deltas and fluvial fans. In total, 40 deltas (Table 1) and 40 fluvial fans (Table 2) were selected from a diverse range of climatic and topographic conditions across the world (Figure 3). Selected deltas exhibit at least one channel bifurcation and two orders of channels. Wave influence in deltas was determined by the presence of straight shorelines with beaches (see Nienhuis et al., 2015), and tide-influence by seaward widening of distributary channels (see Nienhuis et al., 2018). Where both morphological features are present, the deltas are referred to as mixed tide- and wave-influenced deltas (Table 1). A global fluvial fan database

from (Hartley et al., 2010) was utilized to identify modern fans and their apex coordinates. Fluvial fans were selected from different climatic and topographic settings, as well as with different termination styles, such as fans that terminate in terrestrial, playa, lacustrine or ocean environments.

Delta and fluvial fan channel networks were mapped using ArcGIS Pro (Figures 1 and 2). Two feature classes were created: one for deltas and one for fluvial fans. Each delta or fluvial fan landform was then individually mapped as a shapefile layer under the corresponding feature class. The shapefiles were created as polyline features, which allows users to manually trace individual river channel segments while automatically recording line lengths. Channels widths and angles were measured using the line and angle measurement tools. All data was recorded in the attribute table which can be easily copied to an excel document and converted to a python readable csv document.

One drawback associated with using GIS optical imagery data is that we do not know the season during which the images were taken. Fluvial fans and deltas are reactive to changes in precipitation which can cause channel widths to increase during periods of flood flow. None of the selected systems, however, demonstrated a season change across the mapping area. Furthermore, this study only considers values normalized to the initial channel width. Normalizing the data works to decrease the effects of seasonality on channel widths.

#### **e. Climate Data**

Since climate has been suggested to affect bifurcation angles (McCloy, 1970b; Seybold et al., 2017), climate type was tracked for each channel network, initially using the Köppen-Geiger climate classification (Peel et al., 2007), and then simplifying into six hydroclimate types following Hansford and Plink-Björklund (2020). This was done because precipitation variability has been suggested as a significant control for fluvial fan formation (Hansford et al., 2020; Leier et al., 2005). The hydroclimate types group the Köppen-Geiger climate types according to precipitation pattern into tropical rainforest (Af),

monsoonal (Am), humid subtropical (Aw), arid (BWh, BWk BSh, BSk), temperate (Cs, Cw, Cfa, Cfb, Cfc), cold (Dfa), and cold & polar (Ds, Dw, Dfb, Dfc, Dfd, ET, EF) climates (Hansford et al., 2020).

#### **f. Code and Statistics**

Data analysis and visualization was performed using Python. Open-source data visualization libraries Matplotlib (Hunter, 2007), NumPy (Harris et al., 2020), SciPy (Virtanen et al., 2020) and Seaborn (Waskom, 2021) were utilized. Data analyses confidence intervals were calculated according to Mendenhall et al., (2012). Student's T-tests were applied to width, length, and angle values to compare the means of delta and fluvial fan metric distributions. T-tests are used to test the hypothesis that the mean of Gaussian-distributed populations is different by generating a p-value (Trauth, 2006). F-tests were also applied to test for differences between data set variances. F-tests also generate a p-value. For this study, a p-value less than 0.05 (5% significant level) suggests that the two population means and variances are not equal.

## 4. Results

### a. Bifurcation and Divergence/Cross-Over Angles

The average measured delta channel bifurcation angle is  $74.9^\circ$  with a 95th percentile confidence interval of  $\pm 2.4^\circ$  (Figure 6a). The average bifurcation angle in arctic deltas (defined as Cold & Polar: Ds, Dw, Dfb, Dfc, Dfd, ET, EF) is  $78.5 \pm 3.5^\circ$ , while non-arctic deltas have an average bifurcation angle of  $71.8 \pm 3.07^\circ$ . A difference in means between arctic and non-arctic deltas is demonstrated by a t-test ( $p = 0.0012$ ), however a f-test shows that both distributions exhibit similar variances ( $p = 0.47$ ). The average fluvial fan channel divergence/crossover angle is  $55.1^\circ \pm 2.06^\circ$  (Figure 6b). The p-value for a t-test between delta and fluvial fan channel networks angles is  $p = 9.5 \times 10^{-25}$ , which suggests that the average angle values in deltas and fluvial fans are different. The f-test p-value ( $p = 0.57$ ) for delta bifurcation angles and fluvial fan cross-over angles suggests that the variances for these distributions are not significantly different. The distribution of delta bifurcation angles exhibits a slightly larger variance (standard deviation) of  $22.2^\circ$  than in the distribution of fluvial fan divergence/crossover angles where the variance is  $19.6^\circ$ .

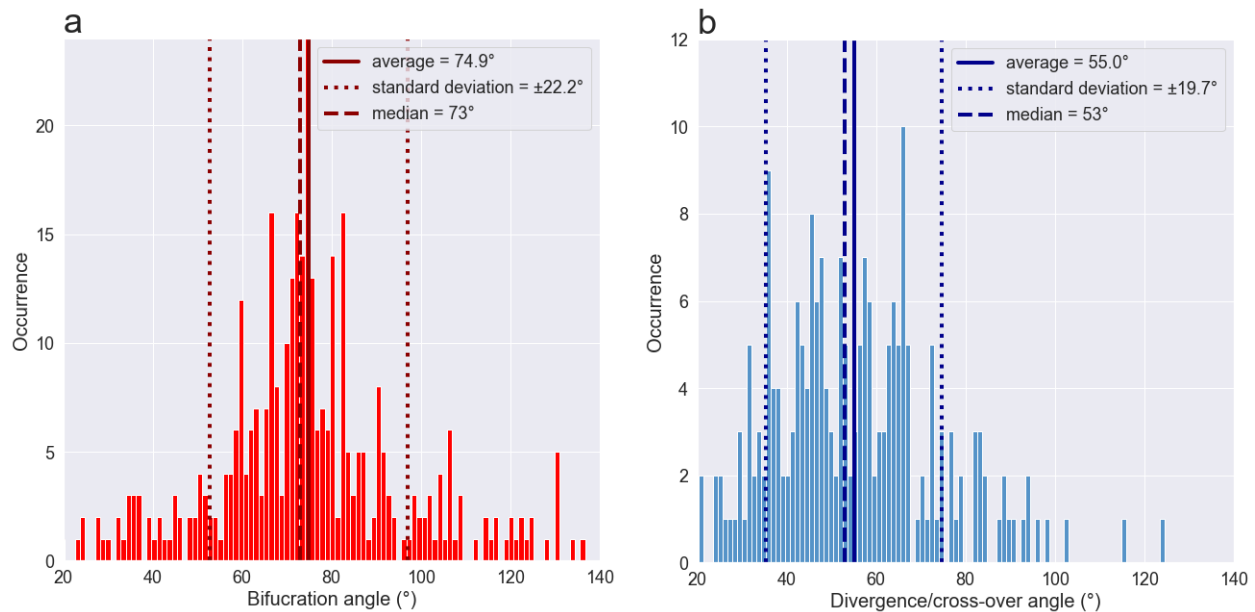


Figure 6: Distribution of (a) delta bifurcation angles and (b) fluvial fan divergence/cross-over angles.

Grouping delta channel bifurcation angles by delta type (river-dominated, tide-influenced, wave-influenced, and mixed tide- and wave-influenced) shows that there is only minor variation between different types of deltas (Figure 7a). The river-dominated deltas in this dataset ( $n = 195$ ) maintain an average bifurcation angle of  $78.2^\circ \pm 3.9^\circ$ . The average for the tide-influenced deltas ( $n = 106$ ) is  $70.9^\circ \pm 3.6^\circ$ , for wave-influenced deltas ( $n = 31$ )  $66.7^\circ \pm 3.3^\circ$ , and for the mixed wave- and tide-influenced deltas ( $n = 31$ )  $75.9^\circ \pm 3.8^\circ$  (Figure 7a). All relationships report an f-test p-value greater than 0.05. However, the f-test p-values between wave-influenced and river-dominated deltas ( $p = 0.0077$ ) as well as tide-influence and river-dominated deltas ( $p = .0057$ ) maintain suggesting differences in mean values).

The distribution of bifurcation angles grouped by order (Figure 8a) shows in deltas that the average bifurcation angle slightly increases from  $70^\circ \pm 3.50^\circ$  and  $69.8^\circ \pm 3.50^\circ$  for first and second order bifurcation to  $77.0^\circ \pm 3.84^\circ$ ,  $76.9^\circ \pm 3.84^\circ$ ,  $76.8^\circ \pm 3.84^\circ$ ,  $77.3^\circ \pm 3.87^\circ$ , and  $78.0^\circ \pm 3.90^\circ$  for bifurcations orders 3 to 7, respectively. Bifurcation order eight exhibits the highest mean angle of  $87.5^\circ \pm 4.38^\circ$  (Figure 8a), however the sample size for this order is low ( $n = 4$ ). In fluvial fans there is no trend in divergence/crossover angles by order (Figure 8b) but the values vary between  $43.3^\circ \pm 2.2^\circ$  ( $n = 4$ ) for playa-termination fans and  $57.4^\circ \pm 2.8^\circ$  ( $n = 5$ ) for lake-termination fans. The average divergence/cross-over angle for ocean-termination fans is  $54.3^\circ \pm 2.7^\circ$  ( $n = 6$ ) and  $56.5^\circ \pm 2.8^\circ$  for terrestrial-termination fans ( $n = 25$ ).

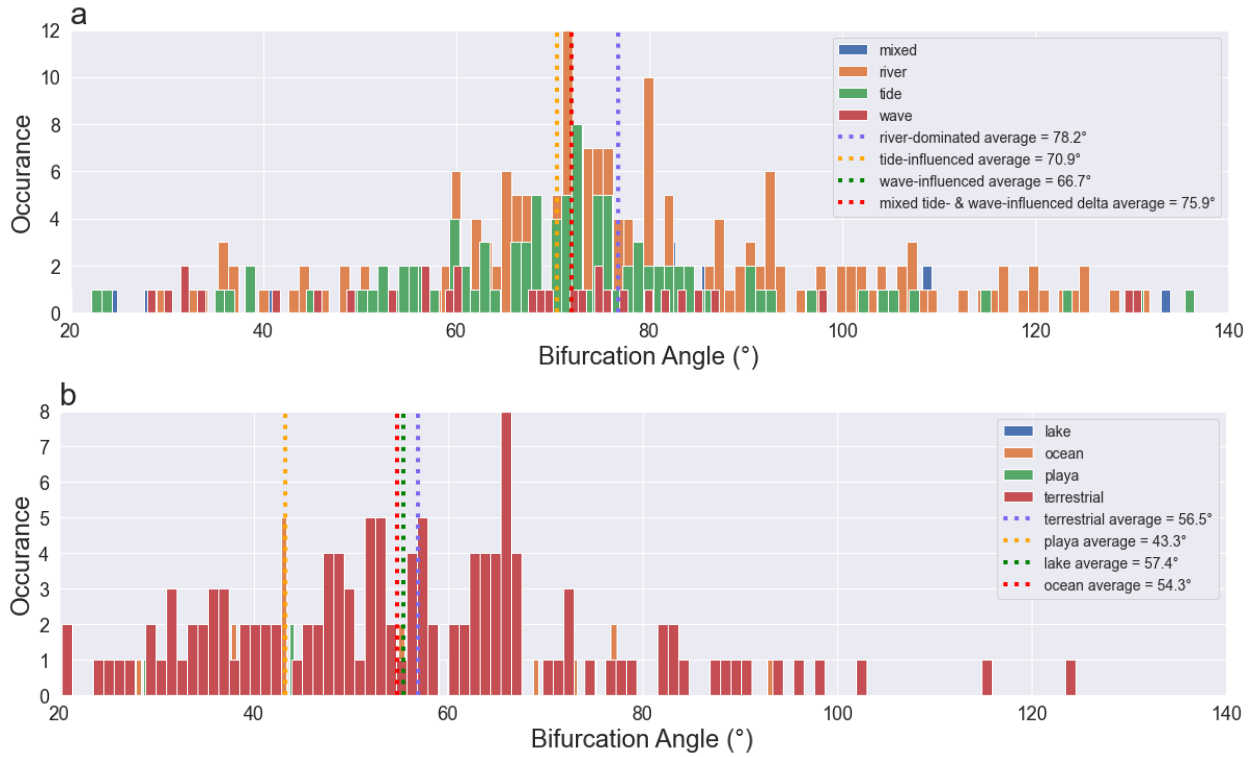


Figure 7: (a) Bifurcation angle distribution by delta type. (b) Divergence/cross-over angle distribution by fluvial fan termination type.

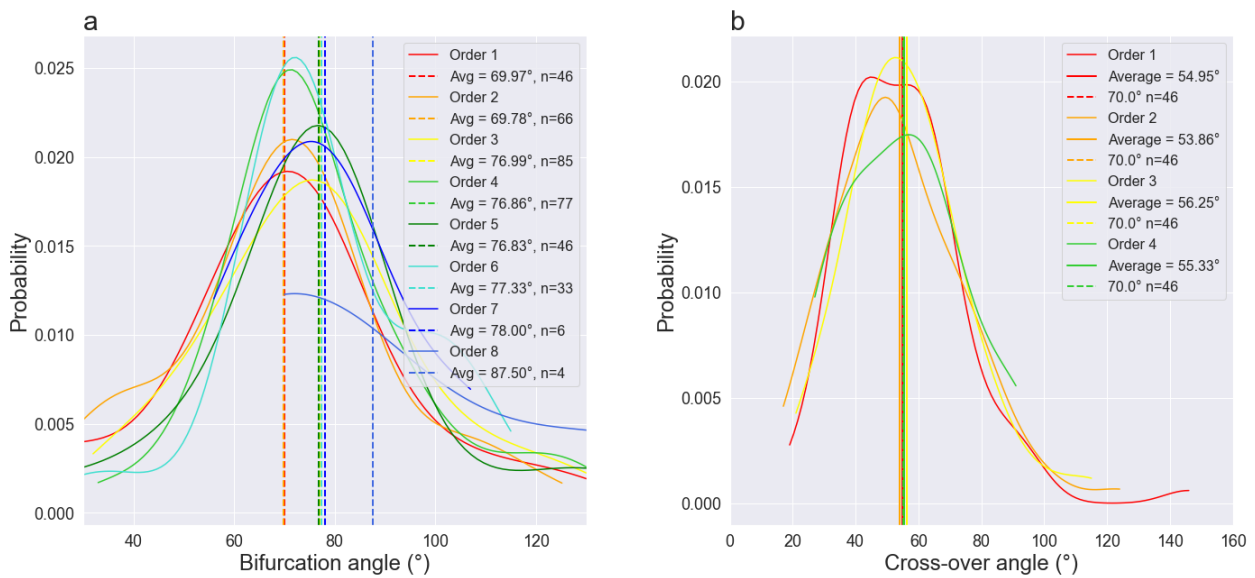


Figure 8: Distribution of (a) delta bifurcation angles, and (b) fluvial fan divergence/cross-over angles.

## **b. Channel Lengths and Widths**

Normalized delta and fluvial fan channel lengths and widths both demonstrate systematic non-linear decreases with increasing channel order (Figure 9). Delta normalized channel lengths are multiple orders of magnitude shorter than normalized channel lengths in fluvial fans (Figures 9a and 9c). There is also a statistically significant difference between the normalized lengths of channels in deltas and fluvial fans. This difference in average length values is supported by a t-test ( $p = 6.78 \times 10^{-71}$ ), however f-test results suggest dissimilarity in the population variance between delta and fluvial fan channel lengths ( $p = 6.88 \times 10^{-58}$ ). Normalized channel width values between deltas and fluvial fans (Figures 9b and 9d) do not demonstrate any separation between their average values ( $p = 0.60$ ), with a f-test value of ( $p = 0.75$ ) suggesting similar population variances for normalized channel width distributions. For delta channel normalized widths (Figure 9a) eighth and ninth order channels exhibit a minor increase in their normalized width values. Most delta channel networks do not achieve eighth and ninth order channels, and these higher order channels have a very small sample size ( $n = 14$  and  $n = 8$ , respectively). Delta channel normalized lengths (Figure 9b) do not demonstrate any change in length trends for these 8th and 9th order channels, nor do fluvial fan channel widths and lengths (Figures 9c and 9d).

Delta normalized channel width and length values grouped by delta type (Figures 10a and 10b) exhibit trends with respect to increasing channel order. River-dominated ( $n = 393$ ) and mixed wave- and tide-influenced deltas ( $n = 69$ ) contain eighth and ninth order channels (Figures 10a and 10b). Tide-influenced deltas ( $n = 218$ ) exhibit a maximum of seventh order channels, while wave-influenced deltas ( $n = 70$ ) contain a maximum of sixth order channels (Figures 10a and 10b). Tide-influenced deltas have the widest channels for a given channel order (Figure 10a), while river-dominated and mixed-energy deltas have the narrowest channels for a given order. Mixed-influenced deltas have the longest channel lengths for a given channel order (Figure 10b).

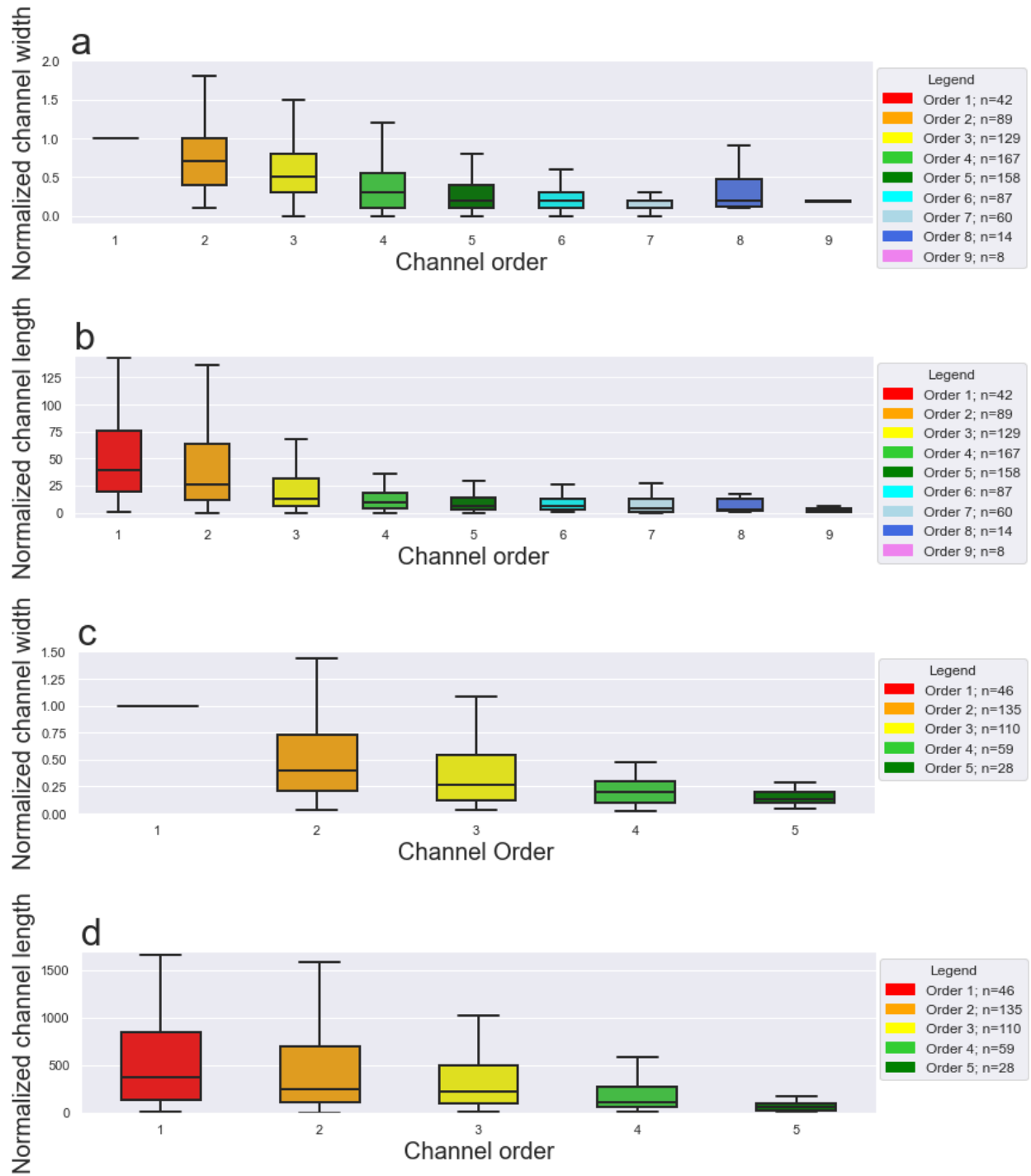


Figure 9: Box and whisker plots illustrating normalized delta channel widths (a) and lengths (b), and normalized fluvial fan channel widths (c) and length (d), plotted by channel order

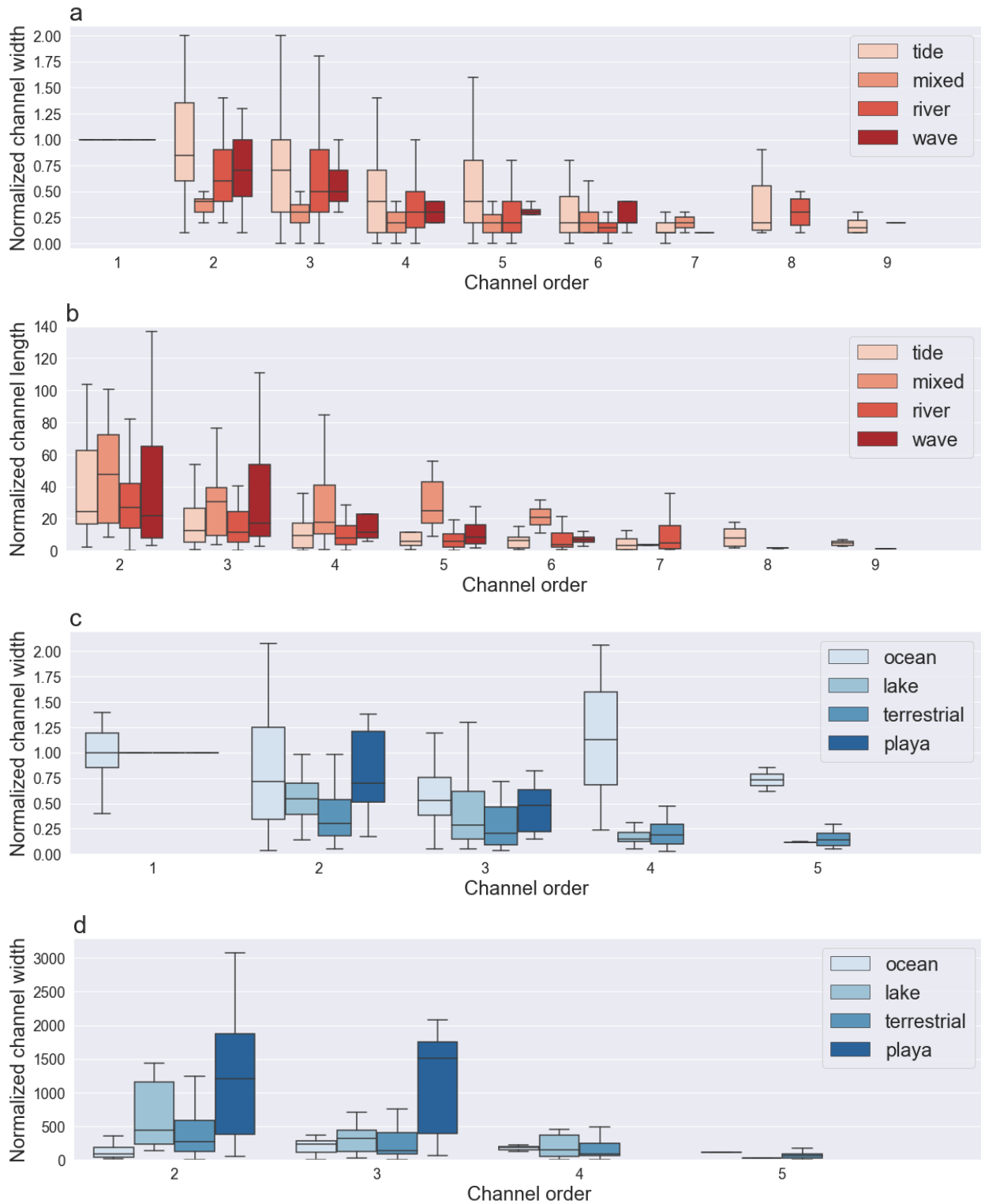


Figure 10: Normalized channel widths and lengths by order for deltas and fluvial fans. (a) Normalized delta channel widths versus channel orders by delta type. (b) Normalized delta channel widths versus channel orders by delta type. (c) Normalized fluvial fan channel widths versus channel orders by fluvial fan termination type. (d) Normalized fluvial fan channel lengths versus channel orders by fluvial fan termination type.

### **c. Fluvial Fans with Downstream Deltas**

In fluvial fans with downstream deltas where the fans enter standing bodies of water t-test results show a difference between both average channel bifurcation and divergence/crossover angles ( $p = 5.93 \times 10^{-5}$ ) and average normalized channel lengths ( $p = 1.05 \times 10^{-14}$ ). Average normalized channel widths in fluvial fans with downstream deltas do not show difference between their means ( $p = 0.78$ ). F-tests show no difference in variances for these normalized channel length/width and bifurcation/divergence angle values  $p = 0.90$ ,  $p = 1.0$ , and  $p = 0.76$ ). It is important to note that these tests of fluvial fans with downstream deltas have a low sample size ( $n=2$ ).

### **d. Hydroclimate**

In fluvial fans, there is a weak ( $>0.5$ ) positive correlation between hydroclimate and the number of channels, number of divergences, and maximum order channels. In deltas, this positive correlation is even weaker ( $<0.29$ ).

## **5. Discussion**

### **a. Morphometric Criteria for Distinguishing Deltas and Fluvial Fans**

Here we show that deltaic and fluvial fan channel networks are distinct, and provide quantitative morphometric criteria for their recognition on Earth and other planetary bodies. Using the largest number of modern deltas thus far, our results confirm the previously proposed deltaic morphometrics of mean bifurcation angle of approximately  $72^\circ$  in deltas (Coffey & Shaw, 2017), and of the fractal pattern of decreasing channel widths and lengths associated with increasing bifurcation orders (Edmonds & Slingerland, 2007; Seybold et al., 2007; Wolinsky et al., 2010).

While the  $72^\circ$  average bifurcation angle has a theoretical explanation in diffusion in non-channelized flow (Coffey & Shaw, 2017), there is currently no theoretical explanation for the  $55^\circ$  average

diversion/crossover angle. While understanding this angle requires further work and is outside of the scope of this paper, there may be a relationship with fan downstream gradient.

The statistically significant difference with the here established fluvial fan divergence/crossover angle of approximately  $55^\circ$  further corroborates the differences in the morphodynamics of these two landforms. Although the nodal avulsions have been established as the mechanism of fluvial fan formation (Assine, 2005; North & Warwick, 2007; Chakraborty et al., 2010), early work on fluvial fans (Friend, 1978; Kelly & Olsen, 1993) and some more recent work (Weissman et al., 2010) suggested bifurcations as an important mechanism of fluvial fan formation. This distinction is important for understanding the upstream vs downstream controls on these landforms, and also for understanding the characteristics of these landforms in the stratigraphic record.

#### **b. Upstream Versus Downstream Controls and Global Change**

Invoking bifurcations as a significant mechanism implies downstream controls, such as where channels enter a standing body of water (e.g. Edmonds & Slingerland, 2007). Previously, downstream controls have also been invoked for fluvial fans through base level rise (e.g. Nichols and Fisher, 2007). Our morphometric results however indicate that nodal avulsions form fluvial fans, and thus agree with the suggested upstream controls on fluvial fans (e.g. Assine, 2005; North & Warwick, 2007; Chakraborty et al., 2010). The effect of basinal control on fluvial fans is only the formation of small deltas along the fan fringe (Figure 2a). This implies differences in how deltas and fluvial fans adjust to global change. While both landforms are sensitive to anthropogenic upstream water and sediment supply changes, sea-level rise will affect deltas more directly. Sea-level rise will not just flood the distributary networks but also cause the avulsion node to shift landward due to the landward shift of the backwater zone (Ganti et al., 2014), further decreasing sediment delivery to shorelines and accelerating the effects of sea-level rise. In fluvial

fans, drowning of the fan toes does not affect the avulsion node position and sediment delivery, and fluvial fans are thus less vulnerable to sea-level rise.

### **c. Stratigraphic Record**

This work also helps to explain a discrepancy in some stratigraphic models of fluvial fans. The data indicate that the proximal fans contain amalgamated channel deposits (e.g., Kelly & Olsen, 1993; Nichols and Fisher, 2007; Weissman et al., 2013), consistent with nodal avulsions that produce laterally amalgamated channel successions through shifting channel locations (Chakraborty et al., 2010). However, some of the conceptual plan-view or morphological models (e.g., Kelly and Olsen, 1993; Nichols and Fisher, 2007) imply bifurcations that we show in this work do not determine the topology of fluvial fans.

### **d. Arctic Deltas**

Arctic deltas exhibit a larger average bifurcation angle of 80° degrees, suggesting that environmental controls affect channel morphodynamics. It has been proposed that river deltas in arctic climates have modified channel networks or bifurcations (e.g. McCloy, 1970b; Lauzon et al., 2019; Piliouras et al., 2021). McCloy (1970b) suggested that channels in arctic deltas are more resistant to bifurcation due to strong winds and high levees better constraining the flow. Others show that smaller channels typically remain frozen longer than larger channels restricting discharge (Lauzon et al., 2019; Walker, 1998), which could cause changes to delta channel lengths and widths and bifurcation angles. Ice cover can also restrict overbank water transport thus confining more of the flow in the channel decreasing land aggradation (Lauzon et al., 2019).

## 6. Conclusions

Here we show that river delta and fluvial fan channel networks can be distinguished using quantitative morphometric criteria. These morphometric differences are caused by delta topology primarily generated by channel bifurcations, and fluvial fan topology by nodal avulsions. Deltaic bifurcations result in average bifurcation angles of approximately  $75^\circ$  ( $72^\circ$  without arctic deltas), and fluvial fan avulsions in average divergence/crossover angles of  $55^\circ$ . Arctic deltas diverge with average bifurcation angles of  $80^\circ$  and indicate that arctic environmental controls affect channel morphodynamics. Both channel networks display downstream decrease in channel length and width with channel hierarchy, but fluvial fan channel lengths are orders of magnitude longer than those in deltas.

## **Acknowledgements**

Luke Gezovich thanks the American Association of Petroleum Geologists (AAPG) Foundation and the Society for Sediment Geology (SEPM) for providing funds to support this research. We also want to thank the Rocky Mountain Association of Geologist (RMAG) for their support in covering publication costs. We further thank Kamini Singha and Lesli Wood for their constructive feedback that helped to improve an earlier version of this manuscript.

## **Data Availability Statement**

Morphometric data and accompanying code used for this project in the study are available at Mendeley Data via DOI: [10.17632/29r6fpkshk.1](https://doi.org/10.17632/29r6fpkshk.1). Citation: Luke; Plink-Bjorklund, Piret; Henry, Jack (2023), "Gezovich et al., 2023 - Quantification of delta and fluvial fan channel networks reveals distinct formative processes", Mendeley Data, V1, doi: [10.17632/29r6fpkshk.1](https://doi.org/10.17632/29r6fpkshk.1)]

Version 6.4.8 of the Jupyter notebook (Anaconda) was used for creating and running the python code necessary for analyses and figure generation.

## References

- Anthony, E. J. (2015). Wave influence in the construction, shaping and destruction of river deltas: A review. In *Marine Geology* (Vol. 361, pp. 53–78). Elsevier.  
<https://doi.org/10.1016/j.margeo.2014.12.004>
- Assine, M. L. (2005). River avulsions on the Taquari megafan, Pantanal wetland, Brazil. *Geomorphology*, 70(3-4 SPEC. ISS.), 357–371.  
<https://doi.org/10.1016/j.geomorph.2005.02.013>
- Assine, M. L., Corradini, F. A., Pupim, F. do N., & McGlue, M. M. (2014). Channel arrangements and depositional styles in the São Lourenço fluvial megafan, Brazilian Pantanal wetland. *Sedimentary Geology*, 301, 172–184. <https://doi.org/10.1016/j.sedgeo.2013.11.007>
- Axelsson, V. (1967). The Laitaure Delta: A Study of Deltaic Morphology and Processes. In *Source: Geografiska Annaler. Series A, Physical Geography* (Vol. 49, Issue 1).
- Bates, C. C. (1953). *RATIONAL THEORY OF DELTA FORMATION*^ (Vol. 37, Issue 9).  
[http://pubs.geoscienceworld.org/aapgbull/article-pdf/37/9/2119/4384158/aapg\\_1953\\_0037\\_0009\\_2119.pdf](http://pubs.geoscienceworld.org/aapgbull/article-pdf/37/9/2119/4384158/aapg_1953_0037_0009_2119.pdf)
- Bentley, S. J., Blum, M. D., Maloney, J., Pond, L., & Paulsell, R. (2016). The Mississippi River source-to-sink system: Perspectives on tectonic, climatic, and anthropogenic influences, Miocene to Anthropocene. In *Earth-Science Reviews* (Vol. 153, pp. 139–174). Elsevier B.V.  
<https://doi.org/10.1016/j.earscirev.2015.11.001>
- Blair, T. C., & Mcpherson, J. G. (1994). *ALLUVIAL FANS AND THEIR NATURAL DISTINCTION FROM RIVERS BASED ON MORPHOLOGY, HYDRAULIC PROCESSES, SEDIMENTARY PROCESSES, AND FACIES ASSEMBLAGES*. <http://pubs.geoscienceworld.org/sepm/jsedres/article-pdf/64/3a/450/2811597/450.pdf>
- Blum, M. D., & Roberts, H. H. (2009). Drowning of the Mississippi Delta due to insufficient sediment supply and global sea-levelrise. In *Nature Geoscience* (Vol. 2, Issue 7, pp. 488–491).  
<https://doi.org/10.1038/ngeo553>
- Bryant, M., Falk, P., & Paola, C. (1995). *Experimental study of avulsion frequency and rate of deposition*. <http://pubs.geoscienceworld.org/gsa/geology/article-pdf/23/4/365/3515841/i0091-7613-23-4-365.pdf>
- Carmichael, M. J., Inglis, G. N., Badger, M. P. S., Naafs, B. D. A., Behrooz, L., Remmelzwaal, S., Monteiro, F. M., Rohrssen, M., Farnsworth, A., Buss, H. L., Dickson, A. J., Valdes, P. J., Lunt, D. J., & Pancost, R. D. (2017). Hydrological and associated biogeochemical consequences of rapid global warming during the Paleocene-Eocene Thermal Maximum. In *Global and Planetary Change* (Vol. 157, pp. 114–138). Elsevier B.V.  
<https://doi.org/10.1016/j.gloplacha.2017.07.014>
- Chakraborty, T., Kar, R., Ghosh, P., & Basu, S. (2010). Kosi megafan: Historical records, geomorphology and the recent avulsion of the Kosi River. *Quaternary International*, 227(2), 143–160. <https://doi.org/10.1016/j.quaint.2009.12.002>

- Chatanantavet, P., & Lamb, M. P. (2014). Sediment transport and topographic evolution of a coupled river and river plume system: An experimental and numerical study. *Journal of Geophysical Research: Earth Surface*, *119*(6), 1263–1282. <https://doi.org/10.1002/2013JF002810>
- Chatanantavet, P., Lamb, M. P., & Nittrouer, J. A. (2012). Backwater controls of avulsion location on deltas. *Geophysical Research Letters*, *39*(1). <https://doi.org/10.1029/2011GL050197>
- Coffey, T. S., & Shaw, J. B. (2017). Congruent Bifurcation Angles in River Delta and Tributary Channel Networks. *Geophysical Research Letters*, *44*(22), 11,427-11,436. <https://doi.org/10.1002/2017GL074873>
- Davidson, S. K., Hartley, A. J., Weissmann, G. S., Nichols, G. J., & Scuderi, L. A. (2013). Geomorphic elements on modern distributive fluvial systems. *Geomorphology*, *180–181*, 82–95. <https://doi.org/10.1016/j.geomorph.2012.09.008>
- De Toffoli, B., Plesa, A. C., Hauber, E., & Breuer, D. (2021). Delta Deposits on Mars: A Global Perspective. *Geophysical Research Letters*, *48*(17). <https://doi.org/10.1029/2021GL094271>
- DeCelles, P. G., & Cavazza, W. (1999). A comparison of fluvial megafans in the Cordilleran (Upper Cretaceous) and modern Himalayan foreland basin systems. *GSA Bulletin*, *111*(9), 1315–1334.
- Devauchelle, O., Petroff, A. P., Seybold, H. F., & Rothman, D. H. (2012). Ramification of stream networks. *Proceedings of the National Academy of Sciences of the United States of America*, *109*(51), 20832–20836. <https://doi.org/10.1073/pnas.1215218109>
- di Achille, G., & Hynek, B. M. (2010). Ancient ocean on Mars supported by global distribution of deltas and valleys. *Nature Geoscience*, *3*(7), 459–463. <https://doi.org/10.1038/ngeo891>
- Dong, T. Y., Nittrouer, J. A., Il'icheva, E., Pavlov, M., McElroy, B., Czapiga, M. J., Ma, H., & Parker, G. (2016). Controls on gravel termination in seven distributary channels of the Selenga River Delta, Baikal Rift basin, Russia. *Bulletin of the Geological Society of America*, *128*(7), 1297–1312. <https://doi.org/10.1130/B31427.1>
- Donselaar, M. E., Cuevas Gozalo, M. C., & Moyano, S. (2013). Avulsion processes at the terminus of low-gradient semi-arid fluvial systems: Lessons from the Río Colorado, Altiplano endorheic basin, Bolivia. *Sedimentary Geology*, *283*, 1–14. <https://doi.org/10.1016/j.sedgeo.2012.10.007>
- Edmonds, D. A., Paola, C., Hoyal, D. C. J. D., & Sheets, B. A. (2011). Quantitative metrics that describe river deltas and their channel networks. *Journal of Geophysical Research: Earth Surface*, *116*(4). <https://doi.org/10.1029/2010JF001955>
- Edmonds, D. A., & Slingerland, R. L. (2007). Mechanics of river mouth bar formation: Implications for the morphodynamics of delta distributary networks. *Journal of Geophysical Research: Earth Surface*, *112*(2). <https://doi.org/10.1029/2006JF000574>
- Fagherazzi, S., Edmonds, D. A., Nardin, W., Leonardi, N., Canestrelli, A., Falcini, F., Jerolmack, D. J., Mariotti, G., Rowland, J. C., & Slingerland, R. L. (2015). Dynamics of river mouth deposits. In

*Reviews of Geophysics* (Vol. 53, Issue 3, pp. 642–672). Blackwell Publishing Ltd.  
<https://doi.org/10.1002/2014RG000451>

- Fagherazzi, S., Hannion, M., & D'Odorico, P. (2008). Geomorphic structure of tidal hydrodynamics in salt marsh creeks. *Water Resources Research*, *44*(2).  
<https://doi.org/10.1029/2007WR006289>
- Farley, K. A., Williford, K. H., Stack, K. M., Bhartia, R., Chen, A., de la Torre, M., Hand, K., Goreva, Y., Herd, C. D. K., Hueso, R., Liu, Y., Maki, J. N., Martinez, G., Moeller, R. C., Nelessen, A., Newman, C. E., Nunes, D., Ponce, A., Spanovich, N., ... Wiens, R. C. (2020). Mars 2020 Mission Overview. In *Space Science Reviews* (Vol. 216, Issue 8). Springer Science and Business Media B.V. <https://doi.org/10.1007/s11214-020-00762-y>
- Fontana, A., Mozzi, P., & Marchetti, M. (2014). Alluvial fans and megafans along the southern side of the Alps. In *Sedimentary Geology* (Vol. 301, pp. 150–171).  
<https://doi.org/10.1016/j.sedgeo.2013.09.003>
- Friend, P. F. (1978). *DISTINCTIVE FEATURES OF SOME ANCIENT RIVER SYSTEMS*.
- Galloway, E. (1975). Process Framework for Describing the Morphologic and Stratigraphic Evolution of Deltaic Depositional Systems. *Deltas: Models for Exploration, 1975*, 87–98.
- Ganti, V., Chu, Z., Lamb, M. P., Nittrouer, J. A., & Parker, G. (2014). Testing morphodynamic controls on the location and frequency of river avulsions on fans versus deltas: Huanghe (Yellow River), China. *Geophysical Research Letters*, *41*(22), 7882–7890.  
<https://doi.org/10.1002/2014GL061918>
- Geleynse, N., Storms, J. E. A., Walstra, D. J. R., Jagers, H. R. A., Wang, Z. B., & Stive, M. J. F. (2011). Controls on river delta formation; insights from numerical modelling. *Earth and Planetary Science Letters*, *302*(1–2), 217–226. <https://doi.org/10.1016/j.epsl.2010.12.013>
- Giosan, L., Syvitski, J., Constantinescu, S., & Day, J. (2014). Climate change Protect the world's deltas. *Nature*, *516*, 31–33.
- Hansford, M. R., & Plink-Björklund, P. (2020). River discharge variability as the link between climate and fluvial fan formation. *Geology*, *48*(10), 952–956. <https://doi.org/10.1130/G47471.1>
- Harris, C. R., Millman, K. J., van der Walt, S. J., Gommers, R., Virtanen, P., Cournapeau, D., Wieser, E., Taylor, J., Berg, S., Smith, N. J., Kern, R., Picus, M., Hoyer, S., van Kerkwijk, M. H., Brett, M., Haldane, A., del Río, J. F., Wiebe, M., Peterson, P., ... Oliphant, T. E. (2020). Array programming with NumPy. In *Nature* (Vol. 585, Issue 7825, pp. 357–362). Nature Research. <https://doi.org/10.1038/s41586-020-2649-2>
- Hartley, A. J., Weissmann, G. S., Nichols, G. J., & Warwick, G. L. (2010). Large distributive fluvial systems: Characteristics, distribution, and controls on development. *Journal of Sedimentary Research*, *80*(2), 167–183. <https://doi.org/10.2110/jsr.2010.016>
- Horton, B. K., & Decelles, P. G. (2001). *Modern and ancient Fluvial megafans in the foreland basin system of the central Andes, southern Bolivia: implications for drainage network evolution in fold-thrust belts*.

- Hunter, J. D. (2007). MATPLOTLIB - 2D GRAPHICS ENVIRONMENT. *Computing in Science & Engineering*.
- Jerolmack, D. J., & Swenson, J. B. (2007). Scaling relationships and evolution of distributary networks on wave-influenced deltas. *Geophysical Research Letters*, *34*(23). <https://doi.org/10.1029/2007GL031823>
- Jones, L. S., & Schumm, S. A. (1999). *Causes of avulsion: an overview* (Vol. 28). Blackwell Science.
- Kelly, S. B., & Olsen, H. (1993). Terminal fans a review with reference to Devonian examples. In *Sedimentary Geology* (Vol. 85).
- Lamb, M. P., Nittrouer, J. A., Mohrig, D., & Shaw, J. (2012). Backwater and river plume controls on scour upstream of river mouths: Implications for fluvio-deltaic morphodynamics. *Journal of Geophysical Research: Earth Surface*, *117*(1). <https://doi.org/10.1029/2011JF002079>
- Langbein, W. B. (1963). The hydraulic geometry of a shallow estuary. *International Association of Scientific Hydrology. Bulletin*, *8*(3), 84–94. <https://doi.org/10.1080/02626666309493340>
- Lauzon, R., Piliouras, A., & Rowland, J. C. (2019). Ice and Permafrost Effects on Delta Morphology and Channel Dynamics. *Geophysical Research Letters*, *46*(12), 6574–6582. <https://doi.org/10.1029/2019GL082792>
- Leier, A. L., DeCelles, P. G., & Pelletier, J. D. (2005). Mountains, monsoons, and megafans. *Geology*, *33*(4), 289–292. <https://doi.org/10.1130/G21228.1>
- Leonardi, N., Canestrelli, A., Sun, T., & Fagherazzi, S. (2013). Effect of tides on mouth bar morphology and hydrodynamics. *Journal of Geophysical Research: Oceans*, *118*(9), 4169–4183. <https://doi.org/10.1002/jgrc.20302>
- Malin, M. C., & Edgett, K. S. (2015). *Evidence for Persistent Flow and Aqueous Sedimentation on Early Mars*. [www.sciencemag.org](http://www.sciencemag.org)
- Marciano, R., Wang, Z. B., Hibma, A., de Vriend, H. J., & Defina, A. (2005). Modeling of channel patterns in short tidal basins. *Journal of Geophysical Research: Earth Surface*, *110*(1). <https://doi.org/10.1029/2003JF000092>
- McCloy, J. M. (1970a). Hydrometeorological Relationships and Their Effects on the Levees of a Small Arctic Delta. *Geografiska Annaler: Series A, Physical Geography*, *52*(3–4), 223–241. <https://doi.org/10.1080/04353676.1970.11879827>
- McCloy, J. M. (1970b). Hydrometeorological Relationships and Their Effects on the Levees of a Small Arctic Delta. *Geografiska Annaler: Series A, Physical Geography*, *52*(3–4), 223–241. <https://doi.org/10.1080/04353676.1970.11879827>
- Mendenhall, W., Beaver, R. J., & Beaver, B. M. (2012). *Introduction to Probability and Statistics* (14th ed.). Brooks/Cole.
- Mohrig, D., Heller, P. L., Paola, C., & Lyons, W. J. (2000). Interpreting avulsion process from ancient alluvial sequences: Guadalope-Matarranya system (northern Spain) and Wasatch Formation

(western Colorado). In *GSA Bulletin*. <http://pubs.geoscienceworld.org/gsa/gsabulletin/article-pdf/112/12/1787/3383751/i0016-7606-112-12-1787.pdf>

- Moscariello, A. (2018). Alluvial fans and fluvial fans at the margins of continental sedimentary basins: Geomorphic and sedimentological distinction for geo-energy exploration and development. In *Geological Society Special Publication* (Vol. 440, Issue 1, pp. 215–243). Geological Society of London. <https://doi.org/10.1144/SP440.11>
- Nardin, W., Mariotti, G., Edmonds, D. A., Guercio, R., & Fagherazzi, S. (2013). Growth of river mouth bars in sheltered bays in the presence of frontal waves. *Journal of Geophysical Research: Earth Surface*, *118*(2), 872–886. <https://doi.org/10.1002/jgrf.20057>
- Nichols, G. J. (1987). *STRUCTURAL CONTROLS ON FLUVIAL DISTRIBUTARY SYSTEMS-THE LUNA SYSTEM, NORTHERN SPAIN*.
- Nichols, G. J., & Fisher, J. A. (2007). Processes, facies and architecture of fluvial distributary system deposits. In *Sedimentary Geology* (Vol. 195, Issues 1–2, pp. 75–90). <https://doi.org/10.1016/j.sedgeo.2006.07.004>
- Nienhuis, J. H., Ashton, A. D., Edmonds, D. A., Hoitink, A. J. F., Kettner, A. J., Rowland, J. C., & Törnqvist, T. E. (2020). Global-scale human impact on delta morphology has led to net land area gain. *Nature*, *577*(7791), 514–518. <https://doi.org/10.1038/s41586-019-1905-9>
- Nienhuis, J. H., Ashton, A. D., & Giosan, L. (2015). What makes a delta wave-dominated? *Geology*, *43*(6), 511–514. <https://doi.org/10.1130/G36518.1>
- Nienhuis, J. H., Hoitink, A. J. F. T., & Törnqvist, T. E. (2018). Future Change to Tide-Influenced Deltas. *Geophysical Research Letters*, *45*(8), 3499–3507. <https://doi.org/10.1029/2018GL077638>
- North, C. P., & Warwick, G. L. (2007). Fluvial fans: Myths, misconceptions, and the end of the terminal-fan model. *Journal of Sedimentary Research*, *77*(9–10), 693–701. <https://doi.org/10.2110/jsr.2007.072>
- Olariu, C., & Bhattacharya, J. P. (2006). Terminal distributary channels and delta front architecture of river-dominated delta systems. *Journal of Sedimentary Research*, *76*(2), 212–233. <https://doi.org/10.2110/jsr.2006.026>
- Ori, G. G., Marinangeli, L., & Baliva, A. (2000). Terraces and Gilbert-type deltas in crater lakes in Ismenius Lacus and Memnonia (Mars). *Journal of Geophysical Research: Planets*, *105*(E7), 17629–17641. <https://doi.org/10.1029/1999JE001219>
- Orton, G. J., & Reading, H. G. (1993). Variability of deltaic processes in terms of sediment supply, with particular emphasis on grain size. *Sedimentology*, *40*(3), 475–512. <https://doi.org/10.1111/j.1365-3091.1993.tb01347.x>
- Owen, A., Nichols, G. J., Hartley, A. J., Weissmann, G. S., & Scuderi, L. A. (2015). Quantification of a distributive fluvial system: The salt wash fans of the Morrison Formation, SW U.S.A. *Journal of Sedimentary Research*, *85*(5), 544–561. <https://doi.org/10.2110/jsr.2015.35>

- Paola, C., Twilley, R. R., Edmonds, D. A., Kim, W., Mohrig, D., Parker, G., Viparelli, E., & Voller, V. R. (2011). Natural processes in delta restoration: Application to the Mississippi Delta. *Annual Review of Marine Science*, 3, 67–91. <https://doi.org/10.1146/annurev-marine-120709-142856>
- Parker, G., Member, /, Paola, C., Whipple, K. X., & Mohrig, D. (1998). *ALLUVIAL FANS FORMED BY CHANNELIZED FLUVIAL AND SHEET FLOW. I: THEORY*. <http://www.ascelibrary.org>
- Peel, M. C., Finlayson, B. L., & McMahon, T. A. (2007). Updated world map of the Köppen-Geiger climate classification. *Hydrol. Earth Syst. Sci.*, 11, 1633–1644.
- Piliouras, A., Lauzon, R., & Rowland, J. C. (2021). Unraveling the Combined Effects of Ice and Permafrost on Arctic Delta Morphodynamics. *Journal of Geophysical Research: Earth Surface*, 126(4). <https://doi.org/10.1029/2020JF005706>
- Pizzuto, J. E. (1987). Sediment diffusion during overbank flows. *Sedimentology*, 34(2), 301–317. <https://doi.org/10.1111/j.1365-3091.1987.tb00779.x>
- Plink-Björklund, P. (2021). Distributive Fluvial Systems: Fluvial and Alluvial Fans. In *Encyclopedia of Geology* (pp. 745–758). Elsevier. <https://doi.org/10.1016/b978-0-08-102908-4.00015-1>
- Radebaugh, J., Ventra, D., Lorenz, R. D., Farr, T., Kirk, R., Hayes, A., Malaska, M. J., Birch, S., Liu, Z. Y. C., Lunine, J., Barnes, J., le Gall, A., Lopes, R., Stofan, E., Wall, S., & Paillou, P. (2018). Alluvial and fluvial fans on Saturn’s moon Titan reveal processes, materials and regional geology. In *Geological Society Special Publication* (Vol. 440, Issue 1, pp. 281–305). Geological Society of London. <https://doi.org/10.1144/SP440.6>
- Rajiv Sinha. (2009). The great avulsion of Kosi on 18 August 2009. *Current Science*, 97(3), 429–433.
- Saito, Y., Thanawat, J., Chaimanee, N., Jarupongsakul, T., & Syvitski, J. P. M. (2007). *Shrinking Megadeltas in Asia: Sea-level Rise and Sediment Reduction Impacts from Case Study of the Chao Phraya Delta The Holocene Red River Delta, Vietnam View project Global Risks and research priorities for coastal subsidence View project Shrinking Megadeltas in Asia: Sea-level Rise and Sediment Reduction Impacts from Case Study of the Chao Phraya Delta*. <https://www.researchgate.net/publication/234045413>
- Schmitz, B., & Pujalte, V. (2007). Abrupt increase in seasonal extreme precipitation at the Paleocene-Eocene boundary. *Geology*, 35(3), 215–218. <https://doi.org/10.1130/G23261A.1>
- Schumm, S. A. (1977). The fluvial system. *Food and Agriculture Organization of the United Nations*.
- Seybold, H., Andrade, J. S., & Herrmann, H. J. (2007). *Modeling river delta formation* (Vol. 104, Issue 43). [www.pnas.org/cgi/doi/10.1073/pnas.0705265104](http://www.pnas.org/cgi/doi/10.1073/pnas.0705265104)
- Seybold, H., Rothman, D. H., & Kirchner, J. W. (2017). Climate’s watermark in the geometry of stream networks. *Geophysical Research Letters*, 44(5), 2272–2280. <https://doi.org/10.1002/2016GL072089>
- Shaw, J. B., & Mohrig, D. (2014). The importance of erosion in distributary channel network growth, Wax Lake Delta, Louisiana, USA. *Geology*, 42(1), 31–34. <https://doi.org/10.1130/G34751.1>

- Singh, H., Parkash, B., & Gohain, K. (1993). Geology Section, Oil and Natural Gas Commission, ERBC, Nazira (Assam)-785 685. In *Current Research in Fluvial Sedimentology. Sediment. Geol* (Vol. 85).
- Slingerland, R., & Smith, N. D. (2004). River avulsions and their deposits. In *Annual Review of Earth and Planetary Sciences* (Vol. 32, pp. 257–285).  
<https://doi.org/10.1146/annurev.earth.32.101802.120201>
- Syvitski, J. P. M., & Brakenridge, R. G. (2013). Causation and avoidance of catastrophic flooding along the Indus River, Pakistan. *GSA Today*, 23(1), 4–10.  
<https://doi.org/10.1130/GSATG165A.1>
- Syvitski, J. P. M., Kettner, A. J., Overeem, I., Hutton, E. W. H., Hannon, M. T., Brakenridge, G. R., Day, J., Vörösmarty, C., Saito, Y., Giosan, L., & Nicholls, R. J. (2009). Sinking deltas due to human activities. *Nature Geoscience*, 2(10), 681–686. <https://doi.org/10.1038/ngeo629>
- Tejedor, A., Longjas, A., Zaliapin, I., & Fofoula-Georgiou, E. (2015). Delta channel networks: 2. Metrics of topologic and dynamic complexity for delta comparison, physical inference, and vulnerability assessment. *Water Resources Research*, 51(6), 4019–4045.  
<https://doi.org/10.1002/2014WR016604>
- Trampush, S. M., & Hajek, E. A. (2017). Preserving proxy records in dynamic landscapes: Modeling and examples from the Paleocene-Eocene Thermal Maximum. *Geology*, 45(11), 967–970.  
<https://doi.org/10.1130/G39367.1>
- Trauth, M. H. (2006). *MATLAB® Recipes for Earth Sciences*.
- Ventra, D., & Clarke, L. E. (2018). Geology and geomorphology of alluvial and fluvial fans: Current progress and research perspectives. In *Geological Society Special Publication* (Vol. 440, Issue 1, pp. 1–21). Geological Society of London. <https://doi.org/10.1144/SP440.16>
- Virtanen, P., Gommers, R., Oliphant, T. E., Haberland, M., Reddy, T., Cournapeau, D., Burovski, E., Peterson, P., Weckesser, W., Bright, J., van der Walt, S. J., Brett, M., Wilson, J., Millman, K. J., Mayorov, N., Nelson, A. R. J., Jones, E., Kern, R., Larson, E., ... Vázquez-Baeza, Y. (2020). SciPy 1.0: fundamental algorithms for scientific computing in Python. *Nature Methods*, 17(3), 261–272. <https://doi.org/10.1038/s41592-019-0686-2>
- Walker, H. J. (1998). Arctic Deltas. In *Source: Journal of Coastal Research* (Vol. 14, Issue 3).
- Wall, S., Hayes, A., Bristow, C., Lorenz, R., Stofan, E., Lunine, J., le Gall, A., Janssen, M., Lopes, R., Wye, L., Soderblom, L., Paillou, P., Aharonson, O., Zebker, H., Farr, T., Mitri, G., Kirk, R., Mitchell, K., Notarnicola, C., ... Ventura, B. (2010). Active shoreline of Ontario Lacus, Titan: A morphological study of the lake and its surroundings. *Geophysical Research Letters*, 37(5).  
<https://doi.org/10.1029/2009GL041821>
- Wang, J., & Plink-Björklund, P. (2019). Stratigraphic complexity in fluvial fans: Lower Eocene Green River Formation, Uinta Basin, USA. *Basin Research*, 31(5), 892–919.  
<https://doi.org/10.1111/bre.12350>

- Waskom, M. (2021). seaborn: statistical data visualization. *Journal of Open Source Software*, 6(60), 3021. <https://doi.org/10.21105/joss.03021>
- Weissman, G. S., Hartley, A. J., Nichols, G. J., Scuderi, L. A., Olson, M., Buehler, H., & Banteah, R. (2010). *Fluvial form in modern continental sedimentary basins: Distributive fluvial systems*. <https://doi.org/10.1016/j.geo>
- Witek, P. P., & Czechowski, L. (2015). Dynamical modelling of river deltas on Titan and Earth. *Planetary and Space Science*, 105, 65–79. <https://doi.org/10.1016/j.pss.2014.11.005>
- Wolinsky, M. A., Edmonds, D. A., Martin, J., & Paola, C. (2010). Delta allometry: Growth laws for river deltas. *Geophysical Research Letters*, 37(21). <https://doi.org/10.1029/2010GL044592>
- Wood, L. J. (2006). Quantitative geomorphology of the Mars Eberswalde delta. *Bulletin of the Geological Society of America*, 118(5–6), 557–566. <https://doi.org/10.1130/B25822.1>
- Wright, L. D. (1977). *Sediment transport and deposition at river mouths: A synthesis*. <http://pubs.geoscienceworld.org/gsa/gsabulletin/article-pdf/88/6/857/3429515/i0016-7606-88-6-857.pdf>
- Wright, L. D., Coleman, J. M., & Thom, B. G. (1973). *PROCESSES OF CHANNEL DEVELOPMENT IN A HIGH-TIDE-RANGE ENVIRONMENT: CAMBRIDGE GULF-ORD RIVER DELTA, WESTERN AUSTRALIA1*.

## Tables

Table 2.1: Deltas and Apex Coordinates

Name	No.	Delta Type	Apex Latitude	Apex Longitude
Amazon	1.1	Tide-influenced	1.430	-51.971
Atchafalaya	1.2	River-dominated	29.485	91.271
Ayeyarwady	1.3	Tide-influenced	16.404	95.9223
Burderkin	1.4	Mixed tide- and wave- influence	-19.660	147.501
Colorado	1.5	Tide-influenced	31.817	-114.806
Colville	1.6	River-dominated	70.181	-150.916
Danube	1.7	Wave-influenced	45.225	-28.738
Dnipro	1.8	River-dominated	46.556	32.551
Don	1.9	River-dominated	47.131	39.457
Dvina	1.10	Tide-influenced	64.531	40.506
Fly	1.11	Tide-influenced	-8.375	142.931
Godavvari	1.12	Mixed tide- and wave- influence	17.023	81.750
Grijalva	1.13	Wave-influenced	18.573	-92.682
Jequitinhonha	1.14	Wave-influenced	-15.848	-38.869
Khovd	1.15	River-dominated	48.211	92.021
Kolyma	1.16	Tide-influenced	68.806	161.318
Krishna	1.17	Mixed tide- and wave- influence	18.504	36.131
Lena	1.18	River-dominated	72.406	126.695
Mackenzie	1.19	Tide-influenced	68.935	-134.805
Mahakam	1.20	Tide-influenced	-0.582	117.279
Mekong	1.21	Tide-influenced	10.719	105.359
Mississippi	1.22	River-dominated	29.155	-89.251
Niger	1.23	Mixed tide- and wave- influence	5.325	6.423
Orinoco	1.24	Mixed tide- and wave- influence	8.598	-62.234
Paraiba do sul	1.25	Wave-influenced	-21.617	-41.047
Parana	1.26	River-dominated	-33.728	-59.285
Po	1.27	Wave-influenced	44.975	12.049
Purari	1.28	Mixed tide- and wave- influence	-7.505	145.093
Rajang	1.29	Tide-influenced	2.287	-111.819
Red	1.30	Mixed tide- and wave- influence	21.080	105.843
Rioni	1.31	Wave-influenced	42.186	41.709
Rufiji	1.32	Tide-influenced	-7.916	-39.271
Saskatchewan	1.33	River-dominated	54.073	-102.375
Selenge	1.34	River-dominated	52.152	106.569
Sinu	1.35	Wave-influenced	9.417	-75.925
Slave	1.36	River-dominated	61.278	-113.589
Volga	1.37	River-dominated	46.736	47.852
Wax lake	1.38	River-dominated	29.540	-91.430
Yukon	1.39	River-dominated	62.492	-163.859
Zambezi	1.40	Mixed tide- and wave- influence	-18.510	-6.134

Table 2.2: Fluvial Fans and Apex Coordinates. Apex Coordinates from Hartley et al., (2010)

Name	No.	Termination Type	Apex Latitude	Apex Longitude
Aichilik	2.1	Ocean	69.59	-142.967
Asku	2.2	Lake	45.95	78.472
Buyunda	2.3	Terrestrial	62.338	153.115
Canning	2.4	Ocean	69.851	-146.461
Cravo norte	2.5	Terrestrial	6.691	-71.841
Cuando	2.6	Terrestrial	-18.24	23.45
Dzavhan gol	2.7	Lake	48.611	93.189
Gash	2.8	Terrestrial	15.473	36.379
Gede-an-chey	2.9	Terrestrial	40.627	48.257
Gilbert	2.10	Ocean	-17.495	142.271
Golmud he	2.11	Terrestrial	36.308	94.78
Great ruaha	2.12	Lake	-7.367	35.334
Guala	2.13	Terrestrial	29.266	79.548
Hali rud	2.14	Playa	28.687	58.552
Ile	2.15	Lake	44.444	76.725
Kal-e shur	2.16	Playa	35.615	56.255
Karnali	2.17	Terrestrial	28.641	81.282
Kongakut	2.18	Terrestrial	69.538	-141.863
Kosi	2.19	Terrestrial	26.53	86.938
Kur	2.20	Terrestrial	49.548	134.758
Manas	2.21	Terrestrial	26.789	90.962
Mashkhil	2.22	Playa	27.922	63.458
Mimbres	2.23	Terrestrial	32.364	-107.952
Mitchell	2.24	Ocean	-16.355	143.062
Nahr wadi	2.25	Terrestrial	32.928	46.443
Niger	2.26	Terrestrial	13.711	-6.07
Nomhon he	2.27	Terrestrial	36.209	96.385
Okavango	2.28	Playa	-18.858	22.382
Okhota	2.29	Terrestrial	59.558	142.888
Oued el mehaiguene	2.30	Ocean	32.605	2.30
Paraguay	2.31	Terrestrial	-16.566	-57.838
Pastaza	2.32	Terrestrial	-3.098	-76.41
Pilcomayo	2.33	Terrestrial	-21.552	-63.011
Pungue	2.34	Terrestrial	-19.5	34.29
Rud-i shur	2.35	Ocean	32.703	60.528
Saskatchewan	2.36	Lake	53.729	-103.199
Schule he	2.37	Terrestrial	40.045	96.75
Shire	2.38	Terrestrial	-16.243	34.959
Taquari	2.39	Terrestrial	-18.435	-54.911
Terter	2.40	Terrestrial	40.351	46.905

